

## Observation of the $^{11}\text{N}$ Ground State

J. M. Oliveira, Jr.,<sup>1,2</sup> A. Lépine-Szily,<sup>1</sup> H. G. Bohlen,<sup>3</sup> A. N. Ostrowski,<sup>4</sup> R. Lichtenthäler,<sup>1</sup> A. Di Pietro,<sup>4</sup>  
 A. M. Laird,<sup>4</sup> G. F. Lima,<sup>1</sup> L. Maunoury,<sup>5</sup> F. de Oliveira Santos,<sup>5</sup> P. Roussel-Chomaz,<sup>5</sup> H. Savajols,<sup>5</sup>  
 W. Trinder,<sup>5</sup> A. C. C. Villari,<sup>5</sup> and A. de Vismes<sup>5</sup>

<sup>1</sup>*IFUSP-Universidade de São Paulo, CP 66318, 05389-970 São Paulo, Brazil*

<sup>2</sup>*CEBES—Centro de Ciências Exatas, Biológicas e da Saúde, Universidade de Sorocaba, Sorocaba, Brazil*

<sup>3</sup>*Hahn-Meitner-Institut Berlin GmbH, Glienicke Strasse 100, D-14109 Berlin, Germany*

<sup>4</sup>*Department of Physics & Astronomy, University of Edinburgh, Edinburgh, EH9 3JZ United Kingdom*

<sup>5</sup>*GANIL, Bld Henri Becquerel, BP 5027, 14021 Caen Cedex, France*

(Received 16 November 1999)

The ground state of the proton-rich, unbound nucleus  $^{11}\text{N}$  was observed, together with six excited states using the multinucleon transfer reaction  $^{10}\text{B}(^{14}\text{N}, ^{13}\text{B})^{11}\text{N}$  at 30A MeV incident energy at Grand Accélérateur National d'Ions Lourds. Levels of  $^{11}\text{N}$  are observed as well defined resonances in the spectrum of the  $^{13}\text{B}$  ejectiles. They are localized at 1.63(5), 2.16(5), 3.06(8), 3.61(5), 4.33(5), 5.98(10), and 6.54(10) MeV above the  $^{10}\text{C} + p$  threshold. The ground-state resonance has a mass excess of 24.618(50) MeV; the experimental width is smaller than theoretical predictions.

PACS numbers: 21.10.Dr, 25.70.Hi, 27.20.+n

The  $A = 11$  isobaric chain has attracted much attention in recent years. On the neutron-rich side the  $^{11}\text{Li}$  and  $^{11}\text{Be}$  nuclides were found to show a neutron halo. Moreover,  $^{11}\text{Be}$  exhibits the inversion of the normal shell-model order, with a  $1/2^+$  ground state and a  $1/2^-$  first excited state. Recent data [1] and analysis [1–3] of one neutron stripping reactions involving  $^{11}\text{Be}$  suggest a large  $d$ -wave admixture in its ground state, while the recently measured [4] one-neutron knockout from the ground state of  $^{11}\text{Be}$  indicates a dominant  $1s$  single particle character. The extraction of the  $^{11}\text{Be}$  ground-state parentage from the recently measured value of its magnetic moment [5] is very sensitive to the quenching of the single particle magnetic moment. The controversial results on the  $^{11}\text{Be}$  ground-state parentage add new interest to the search [6–8] of the  $1/2^+$  resonance as the ground state of  $^{11}\text{N}$ , its mirror nucleus. The sequential proton decay of the  $^{12}\text{O}$  through the  $^{11}\text{N}$  ground state and the hindrance of its diproton decay—observed by [9]—depends on the position and width of the  $^{11}\text{N}$  ground-state resonance. Theoretical calculations on energies and widths of low lying levels in  $^{11}\text{Be}$  and  $^{11}\text{N}$  have been published recently [10–14].

We have realized at Grand Accélérateur National d'Ions Lourds an experiment to undertake the spectroscopic study of the unbound nucleus  $^{11}\text{N}$ . We used the multinucleon transfer reaction  $^{10}\text{B}(^{14}\text{N}, ^{13}\text{B})^{11}\text{N}$ ; the states of  $^{11}\text{N}$  are observed in the  $^{13}\text{B}$  spectrum. The energies of  $^{11}\text{N}$  resonances are given later on in the paper with respect to the  $^{10}\text{C}_{g.s.} + p$  threshold, the  $Q$  value of this threshold being  $Q = -24.635$  MeV. The  $^{14}\text{N}$  beam had an energy of 30A MeV, and the isotopically enriched  $^{10}\text{B}$  target was a “sandwich” of four targets of  $0.1 \text{ mg/cm}^2$  thickness each. The  $^{10}\text{B}$  targets had some content of  $^{11}\text{B}$  and impurities of  $^{16}\text{O}$  and  $^{12}\text{C}$ . To measure the contribution of these other isotopes to the spectrum, we also performed measurements on an isotopically enriched  $^{11}\text{B}$  target ( $0.2 \text{ mg/cm}^2$ ), a

$\text{Li}_2\text{O}$  target ( $0.15 \text{ mg/cm}^2$ ) evaporated on  $50 \text{ } \mu\text{g/cm}^2$  carbon backing, and on a  $0.2 \text{ mg/cm}^2$  carbon target.

The ejectiles were analyzed by the high-precision magnetic spectrometer SPEG. The laboratory angles subtended by SPEG were  $\theta = 1.2^\circ$  to  $4.5^\circ$  and  $\phi = 0^\circ \pm 2.0^\circ$  in the horizontal and vertical planes, respectively. The standard SPEG detection system was used; it includes two drift chambers, an ionization chamber, and a plastic scintillator for the measurements, respectively, of the focal plane position, the energy loss ( $\Delta E$ ), and the residual energy. The time of flight (TOF) was measured using the fast scintillator signal with respect to the cyclotron radio frequency. The two-dimensional particle identification spectrum ( $Z$  vs  $A/q$ , where  $Z$  and  $A/q$  are calculated from  $\Delta E$  and TOF) allows a clear separation of all mass groups due to its very good resolution.

The reaction products were momentum analyzed by the horizontal and vertical position measurements carried out by the two drift chambers. The positions ( $x, y$ ) and the angles ( $\theta, \phi$ ) of each particle in the focal plane were reconstructed by two position measurements 1.2 m apart. The scattering angles  $\Theta$  were calculated from the measured ( $\theta, \phi$ ) angles; they range from  $1.2^\circ$  to  $4.9^\circ$  and the medium angle was  $3.05^\circ$ . Two-dimensional plots of the focal-plane position versus scattering angle were used to perform the kinematical corrections. The projection of the kinematically corrected spectra on the momentum axis yielded the one-dimensional spectra, which have been analyzed. The momentum and energy calibrations were easily performed with the reactions producing  $^{12}\text{B}$  and  $^{13}\text{B}$  ejectiles on the isotopically enriched  $^{10}\text{B}$  target and also on the  $^{16}\text{O}$ ,  $^{11}\text{B}$ , and  $^{12}\text{C}$  targets, allowing also the precise determination of the  $^{16}\text{O}$  and  $^{11}\text{B}$  contents in the isotopically enriched  $^{10}\text{B}$  target. The two-proton stripping reactions ( $^{14}\text{N}, ^{12}\text{B}$ ) were observed on the different targets and were very useful for the energy calibration.

In Fig. 1 we show the kinematically corrected energy spectra of the  $^{13}\text{B}$  ejectiles measured on  $\text{Li}_2\text{O}$  and  $^{11}\text{B}$  targets, corresponding to the reactions  $^{16}\text{O}(^{14}\text{N}, ^{13}\text{B})^{17}\text{Ne}$ ,  $Q_0 = -34.921$  MeV (upper part), and  $^{11}\text{B}(^{14}\text{N}, ^{13}\text{B})^{12}\text{N}$ ,  $Q_0 = -22.369$  MeV (lower part), respectively. The  $^{12}\text{C}(^{14}\text{N}, ^{13}\text{B})^{13}\text{O}$  reaction has a  $Q$  value of  $-36.810$  MeV; this is in excess of 10 MeV more negative than on  $^{10}\text{B}$ . Therefore the reaction is not contributing in the energy region of interest for  $^{11}\text{N}$ .

The energy spectrum measured on the  $^{11}\text{B}$  target (Fig. 1, lower part) shows several peaks corresponding to well known levels of the  $^{12}\text{N}$  nucleus at 0.00, 0.96, 1.19, 1.80 (very weak), 3.13, 4.14 ( $2^- + 4^-$  doublet), and 5.35 MeV. The two well defined peaks at channels 280 and 260 correspond to the  $^{12}\text{N}$  ground state and to the doublet at  $0.96 + 1.19$  MeV. The observed width (FWHM) of the bound ground-state peak represents our energy resolution of 300 keV. All excited states of  $^{12}\text{N}$  are unbound. The resonances were fitted with Breit-Wigner line shapes calculated with the correct dependence of the width  $\Gamma_\ell(E)$  on the decay energy  $E$  and decay  $\ell$  value; the  $\Gamma_\ell$  values at resonance energy were taken from the literature [15]. In the peak fitting procedure these widths were convoluted with the experimental resolution. The ejectile  $^{13}\text{B}$  has its first particle stable excited states at 3.48, 3.53, 3.68, 3.71, 4.13, and 4.83 MeV [16] and thus a clear "window" of  $\sim 3.5$  MeV width exists between its ground and excited states. The excited states around 3.5 MeV are not resolved with our energy resolution. The best fit to the spectrum of  $^{12}\text{N}$  was obtained by taking both the ground state and the population of an excited state at  $\sim 3.7$  MeV in  $^{13}\text{B}$

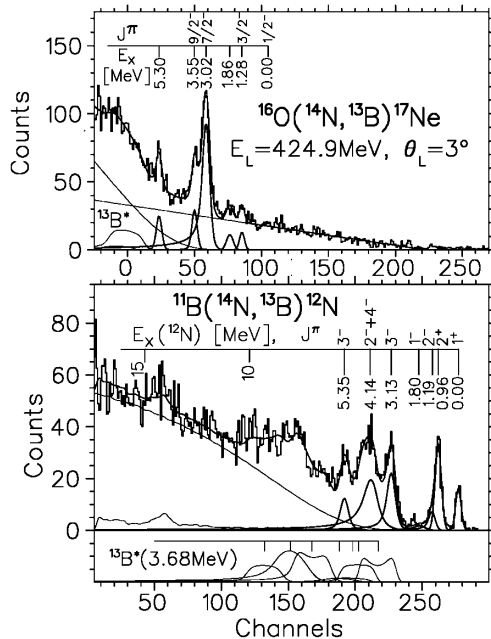


FIG. 1. Energy spectra of the  $(^{14}\text{N}, ^{13}\text{B})$  reactions on  $^{11}\text{B}$  (lower part) and  $^{16}\text{O}$  (upper part) targets used for calibration purposes and for subtraction from the spectrum measured on the  $^{10}\text{B}$  target. See text for details.

into account. In addition, the Doppler broadening due to in-flight  $\gamma$  deexcitation and the line shapes of the corresponding states in  $^{12}\text{N}$  have been treated properly. These  $\gamma$ -broadened lines are shown in the lower part of Fig. 1 separately below the  $x$  axis (thin lines). The different shapes result from variations of the  $\gamma$ -angular distributions described as a sum of different  $m$  substates. The slowly rising background with increasing excitation energy in Fig. 1, lower part, results from the sequential decay  $^{14}\text{C}^* \rightarrow ^{13}\text{B} + p$ . The excitation strength of  $^{14}\text{C}^*$  is obtained in the fit as a broad distribution at 25 MeV excitation energy with a Gaussian form and a width of 7 MeV, which is populated as an intermediate channel  $^{14}\text{C}^* + ^{11}\text{C}$  in a single charge exchange reaction.

On the  $^{16}\text{O}$  target (Fig. 1, upper part) a strong double peak is visible around channel 55 on the energy axis, due to the excitation of the unbound levels at 3.02 and 3.55 MeV in  $^{17}\text{Ne}$  and two lower lying states at 1.28 and 1.87 MeV (a doublet at 1.764 and 1.908 MeV [17]), with the  $^{13}\text{B}$  ejectile in its ground state (thick lines in the fit) or in its excited state at 3.68 MeV (thin lines). The parameters of the background for the sequential decay of  $^{14}\text{C}^* \rightarrow ^{13}\text{B} + p$  have to be the same as in the preceding case and have been kept. A linear background was summed to this in the case of the  $^{16}\text{O}$  target.

The lower part of Fig. 2 shows the energy spectrum of the  $^{13}\text{B}$  ejectiles for the isotopically enriched  $^{10}\text{B}$  target. Contributions of the  $(^{14}\text{N}, ^{13}\text{B})$  reactions on the  $^{16}\text{O}$  and

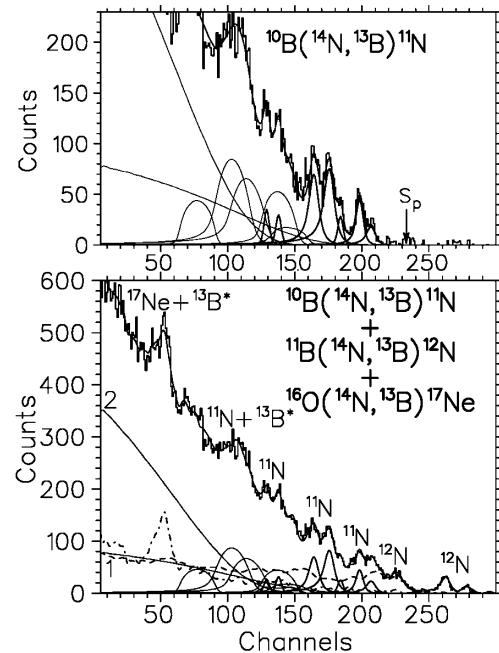


FIG. 2. Lower part: Energy spectrum of  $^{13}\text{B}$  ejectiles measured for the  $(^{14}\text{N}, ^{13}\text{B})$  reaction on the  $^{10}\text{B}$  target containing  $^{11}\text{B}$  and  $^{16}\text{O}$  contaminants. Sequential decay contributions are displayed by curves 1 and 2 (see text). Upper part: The experimental spectrum of the  $^{10}\text{B}(^{14}\text{N}, ^{13}\text{B})^{11}\text{N}$  reaction was obtained by subtraction of normalized experimental spectra obtained with  $^{11}\text{B}$  and  $^{16}\text{O}$  targets, shown in Fig. 1.

$^{11}\text{B}$  impurities in the target can be easily identified, as the first two peaks at channels 280 and 260 due to the  $^{11}\text{B}(^{14}\text{N}, ^{13}\text{B})^{12}\text{N}$  reaction leading to the  $^{12}\text{N}$  ground state and to the doublet at  $0.96 + 1.19$  MeV and the large peak at channel 55 due to the reaction on  $^{16}\text{O}$ . The contribution of the contaminants can be precisely subtracted, since the amount of these impurities can be precisely determined with the corresponding experimental spectra (see Figs. 1 and 2) and also using experimental spectra of the ( $^{14}\text{N}, ^{12}\text{B}$ ) reaction channel (not shown here). All experimental energy spectra, the unsubtracted and the ones to be subtracted, had the same kinematical correction [for the  $^{10}\text{B}(^{14}\text{N}, ^{13}\text{B})^{11}\text{N}$  reaction]. The well defined peaks of the  $^{12}\text{N}$  and  $^{17}\text{Ne}$  recoil nuclei (see Fig. 1) allowed the exact superposition and posterior subtraction of the different spectra. The subtraction of contributions from the  $^{11}\text{B}$  content in the  $^{10}\text{B}$  target is precisely controlled due to the presence of the well defined  $^{12}\text{N}$  peaks at excitation energies of 0.00, 0.96, and 3.13 MeV, where there are no contributions from other target constituents.

The upper part of Fig. 2 shows the final energy spectrum obtained after subtractions of the normalized *experimental* energy spectra obtained with  $^{16}\text{O}$  and  $^{11}\text{B}$  targets. Thus this energy spectrum does not depend on any assumptions used in the fit procedure about excited states of  $^{13}\text{B}$ , and the peaks remaining in the energy spectrum after subtraction are due exclusively to the measured  $^{10}\text{B}(^{14}\text{N}, ^{13}\text{B})^{11}\text{N}$  reaction.

In both parts of Fig. 2 the fit results are shown using (i) Breit-Wigner resonances for the unbound states (thick lines), (ii)  $\gamma$ -recoil broadened lines of mutual excitation of  $^{11}\text{N}$  states and  $^{13}\text{B}$  at 3.68 MeV excitation energy (thin lines), and (iii) the two sequential decay distributions from the proton decay of the broad  $^{14}\text{C}^*$  resonance at 25 MeV ( $\Gamma = 7$  MeV) populated in this case in combination with the ground state (curve 1, Fig. 2) and with the first excited state at 3.35 MeV (curve 2) of the  $^{10}\text{C}$  recoil nucleus. Because of the large ( $\sim 3.5$  MeV) window between the  $^{13}\text{B}$  ground and first excited states, none of the first  $^{11}\text{N}$  resonances, with decay energy less than  $\sim 5$  MeV, can be attributed to excited states of  $^{13}\text{B}$ .

The results of the  $^{10}\text{B}(^{14}\text{N}, ^{13}\text{B})^{11}\text{N}$  reaction are presented in Fig. 3 on a decay energy scale for  $^{11}\text{N}$  with the origin of the energy axis set to the  $^{10}\text{C} + \text{proton}$  decay threshold (with the  $^{13}\text{B}$  ejectile in its ground state). The existence of a peak located on the high energy, right side of the well known  $1/2^-$  first excited state at 2.16 MeV is clear evidence for the observation of the  $^{11}\text{N}$  ground state in this reaction. As we can see in the lower part of Fig. 2, it is situated at channel 206.6, close to the position of the 4.14 MeV peak of  $^{12}\text{N}$  in the contaminant spectrum, but exceeding this peak by about 22 counts per channel. A significance of  $9\sigma$  results for the  $^{11}\text{N}$  ground state. The best fit line shape is calculated with a resonance energy of 1.63 MeV, a width of 400 keV assuming  $\ell = 0$ , and a channel radius of 4.5 fm for the Breit-Wigner resonance. The decay energy of 1.63(5) MeV for the ground-

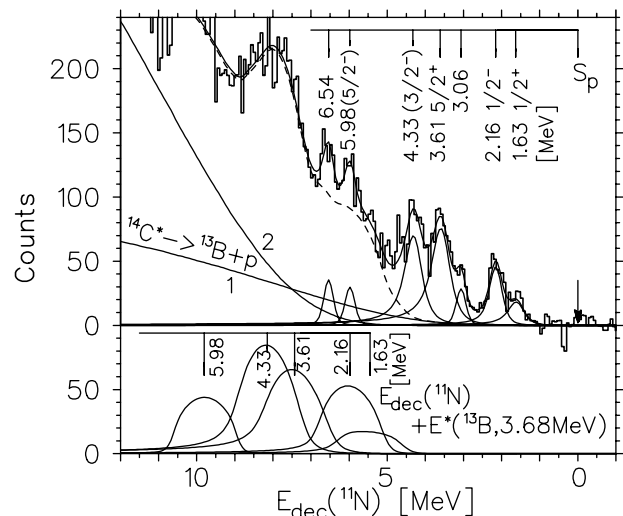


FIG. 3. Energy spectrum of the  $^{10}\text{B}(^{14}\text{N}, ^{13}\text{B})^{11}\text{N}$  reaction obtained after subtraction of the spectra of the contaminants. The arrow indicates the proton threshold.

state resonance corresponds to a mass excess (ME) of  $^{11}\text{N}$  of  $\text{ME} = 24.618(50)$  MeV, allowing the sequential proton decay of  $^{12}\text{O}$ . All other prominent peaks in the spectrum of Fig. 3 up to 6.6 MeV are also resonances of  $^{11}\text{N}$  situated at decay energies of 2.16, 3.06, 3.61, 4.33, 5.98, and 6.54 MeV (Table I). A narrow peak at 3.06 MeV, which is a clearly visible shoulder on the right side of the 3.61 MeV resonance and which has a significance of  $11\sigma$ , is reported for the first time as well as the peak at 6.54 MeV. The peaks at 5.98 and 6.54 MeV are small, but their statistical significance is  $6.4\sigma$  and  $4.9\sigma$ , respectively. The differential cross sections at  $\Theta_{\text{lab}} = 3.05^\circ$  of the  $^{10}\text{B}(^{14}\text{N}, ^{13}\text{B})^{11}\text{N}$  reaction populating the  $^{11}\text{N}$  levels at 1.63, 2.16, 3.06, 3.61, 4.33, 5.98, and 6.54 MeV are 15(5), 28(5), 11(5), 78(15), 63(15), 12(5), and 14(5) nb/sr, respectively.

Comparing the results of the ( $^{14}\text{N}, ^{13}\text{B}$ ) reaction with our recently published results [6] obtained using the  $^{12}\text{C}(^{14}\text{N}, ^{15}\text{C})^{11}\text{N}$  transfer reaction, we can notice that the decay energies obtained for  $^{11}\text{N}$  are very similar in both reactions (see Table I). Moreover in the previous measurement we already had evidence for a narrow state around 3.0 MeV decay energy and a state around 1.5 MeV, but they were credited, respectively, to the population of the  $5/2^+$  (3.63 MeV) and  $1/2^-$  (2.18 MeV) levels of  $^{11}\text{N}$  with the  $^{15}\text{C}$  ejectile in its  $1/2^+$  ground state. There are also important differences between them: the former reaction was more selective, populating intensely only the levels at 2.18 and 3.63 MeV, but with a much higher cross section. In Table I we summarize the decay energies and experimental widths of this work together with results obtained formerly and by other authors.

The search for the  $1/2^+$  ground state of  $^{11}\text{N}$  has intensified in recent times. New experiments [7,8] claim to observe the  $1/2^+$  ground state below the  $1/2^-$  state: Axelsson [7] reports the resonance at 1.3 MeV ( $\Gamma = 0.99$  MeV) and Azhari [8] at 1.45 MeV ( $\Gamma \geq 0.4$  MeV).

TABLE I. Decay energies and widths of  $^{11}\text{N}$  resonances, measured in this work, by our former work [6], by Axelsson *et al.* [7], and compared to theoretical calculations of Fortune *et al.* [10] and Barker [11].

$J^\pi$	This work		Ref. [6]		Ref. [7]		Ref. [10]		Ref. [11]	
	$E_{\text{decay}}$ [MeV]	$\Gamma$ [MeV]	$E_{\text{decay}}$ [MeV]	$\Gamma$ [MeV]	$E_{\text{decay}}$ [MeV]	$\Gamma$ [MeV]	$E_{\text{decay}}$ [MeV]	$\Gamma$ [MeV]	$E_{\text{decay}}$ [MeV]	$\Gamma$ [MeV]
$1/2^+$	1.63(5)	0.4(1)	...	...	1.30(4)	0.99(20)	1.60	1.58	1.40	1.01
$1/2^-$	2.16(5)	0.25(8)	2.18(5)	0.44(8)	2.04	0.69	2.48	0.91	2.21	0.74
	3.06(8)	$\leq 0.10(8)$	(2.92)	(0.1)	...	...	...	...	...	...
$5/2^+$	3.61(5)	0.50(8)	3.63(5)	0.40(8)	3.72	0.6	3.90	0.50	3.88	0.47
$(3/2^-)$	4.33(5)	0.45(8)	4.39(5)	$\leq 0.2(1)$	4.32	0.07				
$(5/2^-)$	5.98(10)	0.10(6)	5.87(15)	0.7(2)	5.5	1.5				
	6.54(10)	0.10(6)								

The  $^{12}\text{N}$  induced single neutron stripping reaction, where the proton decay of the  $^{11}\text{N}$  nucleus is measured [8], yields a peak at 2.24 MeV above the  $^{10}\text{C} + p$  threshold, with a barely separable shoulder at 1.45 MeV. Since the method measures only relative energies, this shoulder could be due to the  $1/2^+$  ground state and/or due to the proton decay of a  $3/2^-$  excited state around 4.6 MeV in  $^{11}\text{N}$  (our resonance at 4.33 MeV) to the first excited  $2^+$  state of  $^{10}\text{C}$  at 3.35 MeV.

The peak at 1.63(5) MeV decay energy in our spectrum (Fig. 3) is the ground-state resonance. In the analysis its width can range between  $\Gamma = 300\text{--}600$  keV for a fit of the experimental spectrum; an optimum value is found at 400 keV using  $\ell = 0$  for the proton decay. A distorted wave Born approximation analysis [1] of recent  $p(^{11}\text{Be}, ^{10}\text{Be})d$  data yielded, respectively, spectroscopic factors of 0.67–0.79 and 0.16–0.22 for the  $[0^+ \otimes s_{1/2}]$  and  $[2^+ \otimes d_{5/2}]$  configurations of the  $^{11}\text{Be}$  ground state, thus a 20%  $d$ -wave admixture. Recent analyses by Johnson and collaborators [2,3] of this and older  $^{10}\text{Be}(d, p)^{11}\text{Be}$  data [18], including the breakup of the deuteron and of the  $^{11}\text{Be}$  in the calculations, arrive at a  $d$ -wave admixture of  $\sim 50\%$  with spectroscopic factors of about 0.2–0.3 for both configurations. If we assume the same spectroscopic factor  $S = 0.2$  for the  $^{11}\text{N}$  ground-state resonance and use  $\Gamma_{\text{sp}} = 2.1$  MeV for the single particle width of an  $s_{1/2}$  resonance 1.60 MeV above the  $^{10}\text{C} + p$  threshold [10], then  $\Gamma_{\text{pred}} = S \cdot \Gamma_{\text{sp}} = 0.4 \pm 0.2$  MeV, in good agreement with our experimental width for the 1.63 MeV ground-state resonance.

The peak at 2.16(5) MeV is the  $1/2^-$  resonance of  $^{11}\text{N}$ , also observed by the other authors [at 2.18(5) MeV in our previous work [6], at 2.24 MeV by Benenson *et al.* [19] and Azhari *et al.* [8], and at 2.04 MeV by Axelsson *et al.* [7]]. The peak at 3.06(8) MeV has a very narrow width and is difficult to assign. The peak at 3.61(5) MeV is the  $5/2^+$  resonance observed at 3.63(5) MeV in our previous work [6] and at 3.72 MeV by [7]. The resonance at 4.33(5) MeV was observed at 4.39(5) MeV in our previous work and at 4.32 MeV by Axelsson [7], while the peak at 5.98(10) MeV was at 5.87(15) MeV in our previous work. A new peak at 6.54(10) MeV has not been observed before. Shell-model calculations [8,20] for  $^{11}\text{N}$

predict a  $K = 1/2$  band, whose  $1/2^-$ ,  $3/2^-$ , and  $5/2^-$  states lie, respectively, at 2.24, 4.61, and 5.7 MeV, and probably can be identified with our observed peaks at 2.16, 4.33, and 5.98 MeV (formerly at 2.18, 4.39, and 5.87 MeV).

We can conclude that by means of the  $^{10}\text{B}(^{14}\text{N}, ^{13}\text{B})^{11}\text{N}$  reaction, we could clearly observe the  $^{11}\text{N}$  ground-state resonance ( $1/2^+$ ) at 1.63 MeV decay energy, followed by six well resolved resonances of  $^{11}\text{N}$  in the spectrum of  $^{13}\text{B}$  ejectiles up to decay energies of 6.54 MeV. In our opinion this is the clearest evidence up to now of the existence and the observation of this long searched for ground state of the  $^{11}\text{N}$  nucleus. Its width is smaller than predicted, but, by analogy with the  $^{11}\text{Be}$  nucleus, one could expect a strong  $d$ -wave admixture in the ground-state wave function of the  $^{11}\text{N}$  nucleus resulting in a smaller width.

We thank Dr. D. J. Millener, Dr. F. Barker, and Dr. R. C. Johnson for enlightening discussions. J. M. O. thanks FAPESP. A. M. L. and A. N. O. thank EPSRC.

- 
- [1] S. Fortier *et al.*, Phys. Lett. B **461**, 22 (1999).
  - [2] R. C. Johnson *et al.*, in *Proceedings of ENPE99, Experimental Nuclear Physics in Europe, Sevilla, Spain, 1999*, edited by B. Rubio, M. Lozano, and W. Gelletly, AIP Conf. Proc. No. 495 (AIP, New York, 1999), p. 297.
  - [3] N. K. Timofeyuk *et al.*, Phys. Rev. C **59**, 1545 (1999).
  - [4] T. Aumann *et al.*, Phys. Rev. Lett. **84**, 35 (2000).
  - [5] W. Geithner *et al.*, Phys. Rev. Lett. **83**, 3792 (1999).
  - [6] A. Lépine-Szily *et al.*, Phys. Rev. Lett. **80**, 1601 (1998).
  - [7] L. Axelsson *et al.*, Phys. Rev. C **54**, R1511 (1996).
  - [8] A. Azhari *et al.*, Phys. Rev. C **57**, 628 (1998).
  - [9] R. A. Kryger *et al.*, Phys. Rev. Lett. **74**, 860 (1995).
  - [10] H. T. Fortune *et al.*, Phys. Rev. C **51**, 3023 (1995).
  - [11] F. C. Barker, Phys. Rev. C **53**, 1449 (1996).
  - [12] S. Grévy *et al.*, Phys. Rev. C **56**, 2885 (1997).
  - [13] F. M. Nunes *et al.*, Nucl. Phys. **A596**, 171 (1996).
  - [14] P. Descouvemont, Nucl. Phys. **A615**, 261 (1997).
  - [15] F. Ajzenberg-Selove, Nucl. Phys. **A433**, 1 (1985).
  - [16] R. Middleton and D. J. Pullen, Nucl. Phys. **51**, 50 (1964).
  - [17] V. Guimarães *et al.*, Phys. Rev. C **58**, 116 (1998).
  - [18] B. Zwieglinski *et al.*, Nucl. Phys. **A315**, 124 (1979).
  - [19] W. Benenson *et al.*, Phys. Rev. C **9**, 2130 (1974).
  - [20] D. J. Millener *et al.*, Phys. Rev. C **28**, 497 (1983).